Journal of
Synchrotron
Radiation

ISSN 0909-0495

Received 2 March 2005
Accepted 28 April 2005

Pure-type superconducting permanent-magnet undulator

Takashi Tanaka,* Rieko Tsuru and Hideo Kitamura

RIKEN/SPring-8, Koto 1-1-1, Mikazuki, Sayo, Hyogo 679-5148, Japan.
E-mail: ztanaka@spring8.or.jp

A novel synchrotron radiation source is proposed that utilizes bulk-type high-temperature superconductors (HTSCs) as permanent magnets (PMs) by *in situ* magnetization. Arrays of HTSC blocks magnetized by external magnetic fields are placed below and above the electron path instead of conventional PMs, generating a periodic magnetic field with an offset. Two methods are presented to magnetize the HTSCs and eliminate the field offset, enabling the HTSC arrays to work as a synchrotron radiation source. An analytical formula to calculate the peak field achieved in a device based on this scheme is derived in a two-dimensional form for comparison with synchrotron radiation sources using conventional PMs. Experiments were performed to demonstrate the principle of the proposed scheme and the results have been found to be very promising.

Keywords: insertion device; bulk HTSC.

1. Introduction

In synchrotron radiation facilities, insertion devices (IDs) such as undulators and wigglers are widely used to improve the performance of the synchrotron radiation. In these devices, strong periodic fields are generated usually by rare-earth permanent magnets (REPMs), and in some cases pole pieces made from a material with high permeability are used to enhance the peak field. The performance of the REPM material is thus important for synchrotron radiation sources and in fact is improved year by year. It should be noted, however, that there is a theoretical limit to the remanent field of the REPM material (Sagawa *et al.*, 1985), which means that the achievable magnetic field in the ID with REPMs will also have a theoretical upper limit.

In order to overcome this limit, pulsed electromagnets (Warren & Fortgang, 1993, and references therein) or superconductors (Ingold *et al.*, 1993*a*; Chouhan *et al.*, 2003; Schlueter *et al.*, 2004) can be used instead of REPMs. In practice, IDs equipped with superconducting coils have been constructed and under development for about 20 years. These superconducting IDs can produce much higher fields than achievable by conventional IDs with REPMs at the same magnet gap. It should be noted, however, that construction and operation of superconducting IDs would be more difficult for shorter periodic lengths to be utilized as undulators since they should operate around liquid-helium temperatures.

There is another way of utilizing superconductors as magnets. Because the resistivity of superconductors is zero, a current loop induced by Faraday's electromagnetic induction law is not damped at all and flows forever (persistent current). Thus, such a 'magnetized' superconductor works as a magnet with a much stronger field than the REPM and is called a superconducting PM (SCPM). In particular, SCPMs made from bulk-type high-temperature superconductors (HTSCs) perform better than REPMs. However, there have been few applications so far because SCPMs should be kept under cryogenic conditions from magnetization to assembly. We have been investigating the possibility of applying such SCPMs to synchrotron radiation sources for the future development of short-period undulators. The most important point is to develop an *in situ* magnetization procedure for the superconductors.

We recently proposed a scheme to utilize SCPMs by *in situ* magnetization to enhance the magnetic field in the IDs with REPMs (Tanaka, Hara *et al.*, 2004), in which ring-shaped HTSCs placed on the REPM blocks are magnetized by opening the magnet gap. This scheme is based on the cryo-undulator concept (Hara *et al.*, 2004), in which the REPMs are cooled to improve the remanent field and coercivity. We carried out experiments to demonstrate the concept of this scheme and found a field enhancement as expected. However, the performance of the HTSCs was found to degrade during the experiments, which might result from mechanical weakness of the ring-shaped HTSCs.

In this paper we propose another SCPM scheme for future development of synchrotron radiation sources, in which rectangular parallelepiped HTSCs are used as SCPMs, and *in situ* magnetization of them is performed without any REPMs. The principle of generating a persistent current for magnetization of SCPMs is similar to that of the so-called 'flux pump' used in the conventional superconducting technology.

2. Principle

Let us consider an array of superconductor blocks as shown in Fig. 1. If these blocks are made from a type-II superconducting material they can be magnetized, *i.e.* a current loop can be generated inside each block. The magnetic field generated by such current loops is composed of a uniform field (field offset) with the polarity determined by the current loop, and a periodic field that reflects the periodic structure of the superconductor array. After elimination of the field offset, the remaining periodic field works as an ID field. Let us call an ID based on this concept a superconducting PM undulator (SCPMU). Fig. 2 shows a schematic illustration of a SCPMU, which consists of superconductor arrays and coils that generate a uniform field. The superconductors are preferably made from HTSCs, so that the operating temperature can be set high enough for the cryocooler to remove the heat load brought by the electron beam.

We have so far found two methods of magnetizing the HTSCs and eliminating the field offset. The first one utilizes the coil surrounding the HTSC array for magnetization and field offset elimination. The second takes advantage of the gap movement for magnetization. The design based on the former method is called type A and that for the latter type B, details of which will be presented in the following sections. Let the critical temperature and current density of the superconductors be T_c and j_c, respectively.

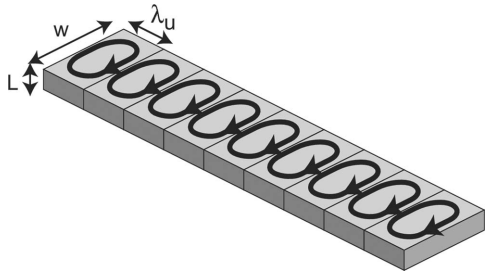

Figure 1
An array of magnetized superconducting blocks that work as PMs.

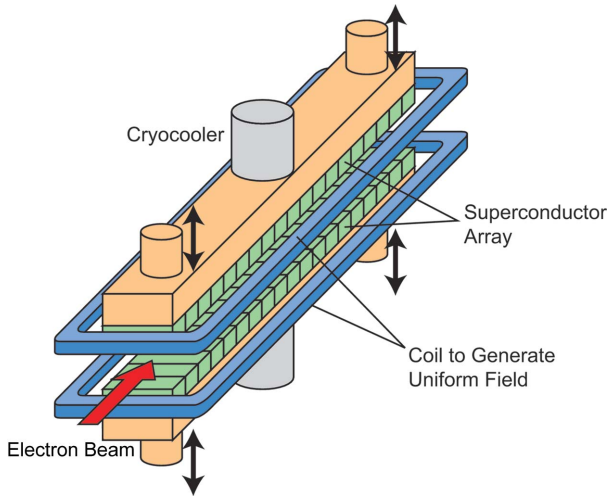

Figure 2
Schematic illustration of the SCPMU.

2.1. Type A

The operation procedure in type A is explained in Fig. 3. At first, the temperature of the HTSCs is kept higher than T_c and the coil is turned on (*a*). The green line indicates the magnetic field distribution at the center of the gap. Then the HTSCs are cooled to a temperature lower than T_c (*b*). When the coil is turned off (*c*), the HTSCs are magnetized in order to keep the flux inside. The magnetized HTSCs generate a periodic magnetic field with a field offset. Finally, the coil is again turned on (*d*) with the polarity reversed and current adjusted to eliminate the field offset.

It should be noted that the magnetic field generated initially by the coil in (*a*) should be so high that the current density of the magnetized HTSCs reaches j_c. Otherwise the field-offset elimination process (*d*) does not work very well. This in turn implies that each HTSC should have a similar j_c value to realise a good field performance as an ID, especially as an undulator.

2.2. Type B

The operation procedure in type B is explained in Fig. 4, in which the top array is shifted by half a period ($\lambda_u/2$) with respect to the bottom array along the longitudinal (z) axis, or *vice versa*. Initially the gap is fully opened and the polarity of the coils is opposite to each other, resulting in no field at the gap center. On the other hand, the HTSCs can be magnetized because they are located far from the gap center and near to one of the coils. In the figure, the magnetic fields near the top and bottom arrays are indicated by the red and blue lines, respectively, while that at the gap center is indicated by the green line. Each HTSC array is magnetized (*c*) as in type A and generates a periodic field with an offset. The field offset is, however, cancelled at the gap center owing to summation of the magnetic fields by the top and bottom arrays resulting in a periodic field without offset. When the gap is closed (*d*), the current density in each HTSC increases until it reaches j_c in order to exclude the magnetic field from the opposite array and to keep the magnetic flux inside. This means that the initial magnetic fields for magnetizing the HTSCs do not have to be necessarily high because they are further magnetized by closing the gap. If the initial field is adjusted so that the current density does not reach j_c, even at the minimum gap, then we can expect a good field distribution with even values of the peak field.

It should be noted that a strong skew quadrupole field is induced using this method, which should be corrected so as not to affect the storage ring operation. The most straightforward way is to install correction magnets at both ends. The surrounding coils used to magnetize the HTSCs can also be used, although the state of the HTSCs will be effected.

Now let us investigate the magnetization process during the gap change. In order to simplify the situation we approximate the current loops in the HTSCs as two current loops placed above and below, as shown in Fig. 5. From symmetry, the currents I flowing in the two long coils are identical except for the polarity. Let the self and mutual inductances of the long

coil be L and M, respectively. The values M and I are functions of the gap g. When the gap is changed from g_1 to g_2 we have an equation to denote the flux change,

$$L[I(g_2) - I(g_1)] = M(g_2)I(g_2) - M(g_1)I(g_1),$$

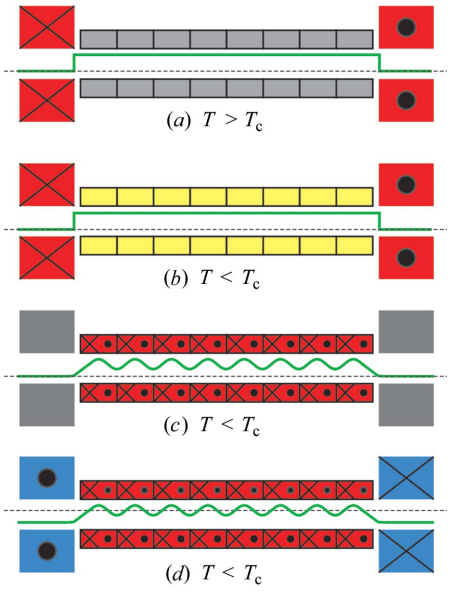

Figure 3
Method for magnetizing the HTSCs and eliminating the field offset in type A.

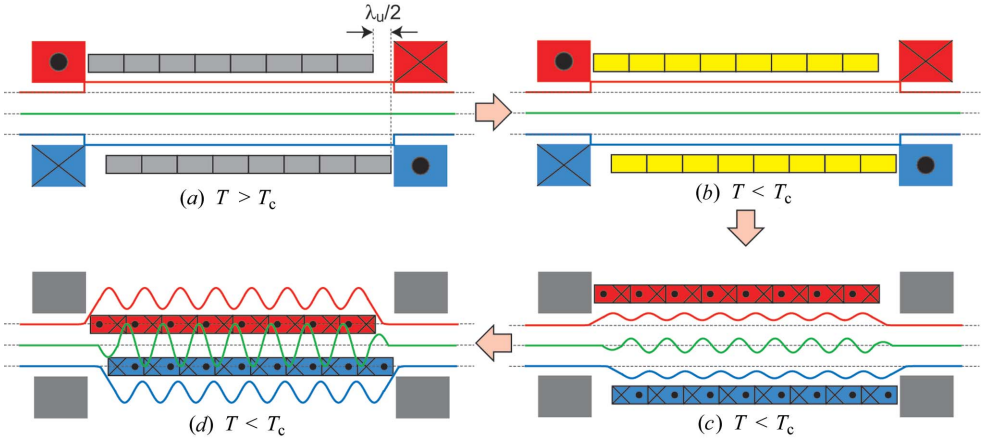

Figure 4
Method for magnetizing the HTSCs and eliminating the field offset in type B.

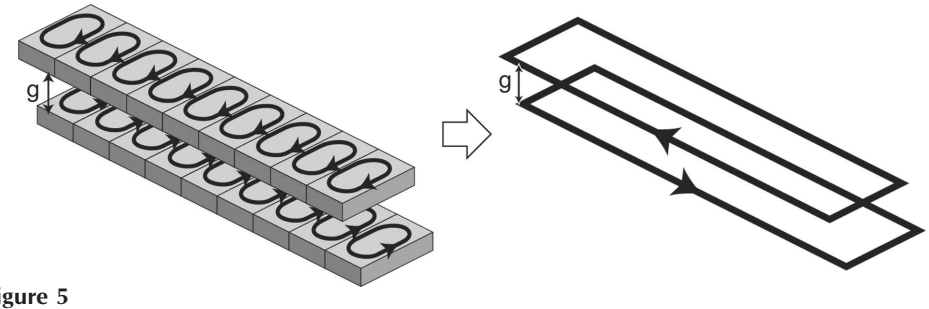

Figure 5
Approximation of current loops as two long current loops.

where the left-hand side and right-hand side denote the flux changes owing to self and mutual inductances, respectively. Now we have a formula to express the current change,

$$I(g_2) = I(g_1)\frac{1 - M(g_1)/L}{1 - M(g_2)/L}.$$

When g_2 approaches 0, $M(g_2)$ approaches L. Thus we expect a large enhancement of the persistent current in the HTSC, *i.e.* the magnetic field.

2.3. Performance

In order to investigate the performance of the SCPMU, let us calculate the magnetic field generated by two HTSC arrays placed with a gap g in between. To simplify the situation we assume that the width (w) of the current loop is infinitely long. In such a case the magnetic fields can be calculated under a two-dimensional approximation (see, for example, Ingold *et al.*, 1993*b*). Substituting the coil dimensions shown in Fig. 1 into equation (6) in Appendix *A* and assuming $2\pi L/\lambda_u \gg 1$, we have the achievable peak field B_p in the SCPMU,

$$B_p = \frac{2\mu_0\lambda_u j_c}{\pi^2}\exp(-\pi g/\lambda_u),$$

where j_c is the critical current density of the HTSC block. In practical units,

$$B_p(T) = 2.55 \times 10^{-4}\lambda_u\,[\text{mm}]\; j_c\,[\text{A/mm}^2]\;\exp(-\pi g/\lambda_u). \quad (1)$$

It should be noted that B_p is proportional to λ_u and j_c, meaning that a HTSC material with high j_c is indispensable for construction of a SCPMU with a short period.

3. Experiments

In order to demonstrate the principle of the SCPMU, we performed experiments using bulk-type HTSCs made from a commercially available material, Gd-Ba-Cu-O ($T_c \simeq 92$ K). The experimental set-up is shown schematically in Fig. 6. Parallelepipedic HTSC blocks, with lengths corresponding to the undulator period λ_u of 10 mm, were fixed onto a copper plate that was connected to the cryocooler head, and inserted into the gap of an electromagnet (normal conducting). The dimensions of the HTSC block are indicated in the figure. The effects owing to the iron yoke of the electromagnet were estimated by calculation and found to be negligible because of the small dimensions of the HTSC block. A cartridge-

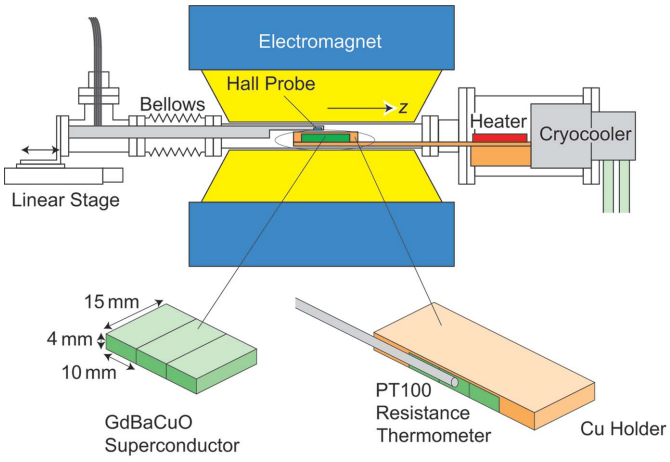

Figure 6
Schematic illustration of the experimental set-up to demonstrate the principle of the SCPMU.

type heater was installed on the copper plate to control the temperature. From the opposite side, a Hall probe fixed on a cantilever was inserted to measure the magnetic field. The cantilever was connected to a linear stage enabling the Hall probe to be scanned in order to measure the field distribution along the z axis. The distance from the Hall probe center to the surface of the HTSC blocks was 1 mm, corresponding to a gap value of 2 mm. The temperatures of the HTSC blocks were measured using a platinum resistance thermometer (PT100) attached to them.

First, we investigated the intrinsic performances of the HTSC block used in the experiments. Only a single HTSC block was fixed onto the copper plate and the magnetic field generated by it was measured by the Hall probe while the coil current of the electromagnet was scanned. The critical current density j_c was determined by comparison with the magnetic field generated by a unit current loop with the same dimensions as the HTSC block, being calculated using a numerical method based on Biot–Savart's law. The results are shown in Fig. 7 for different values of the temperature. We could not determine j_c at temperatures lower than 43 K because magnetization of the HTSC block did not saturate even when the maximum field supplied by the electromagnet was applied. The curve indicated in the figure is calculated using the expression

$$j_c(T) = j_c(0)\left[1 - (T/T_c)^2\right]^m$$

that denotes empirically the relation between j_c and T (Koziol *et al.*, 1994). Using least-squares fitting, $j_c(0)$ and m have been determined to be 2.76 kA mm^{-2} and 2.25, respectively. With these parameters we can expect that j_c reaches 2 kA mm^{-2} at a temperature of 35 K.

Having determined j_c, we measured the magnetic field distribution generated by three HTSC blocks arranged as in Fig. 6. In order to simulate the method for magnetization of HTSCs and elimination of the field offset, we took the following steps:

(i) set the temperature of the HTSCs to 100 K;

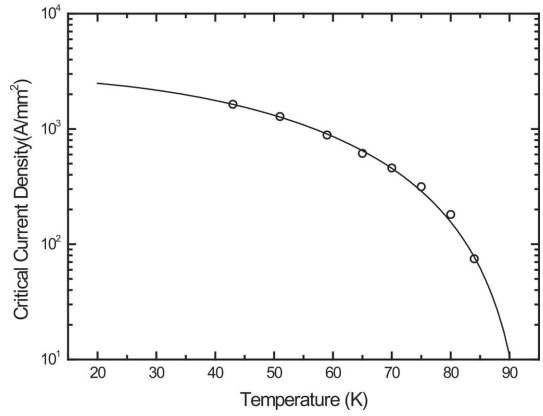

Figure 7
Critical current density j_c of the HTSC block used in the experiments as a function of temperature (empty circles). The solid line shows an empirical curve with parameters m = 2.25 and j_c = 2760 A mm^{-2}.

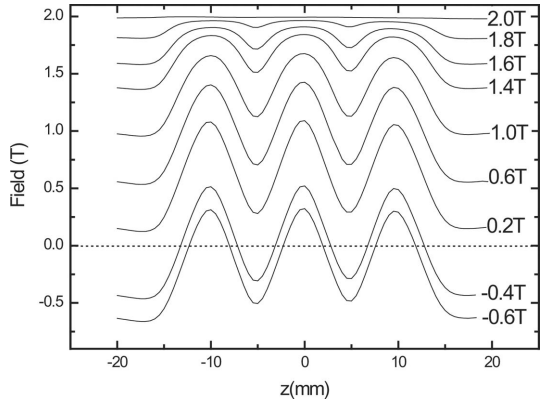

Figure 8
Field distributions measured at 59 K for different values of the magnetic strength of the electromagnet.

(ii) turned on the electromagnet and applied 2 T;

(iii) cooled the HTSCs to a target temperature;

(iv) reduced the magnetic field of the electromagnet (B_e) by 0.2 T and measured the magnetic field distribution;

(v) repeated step (iv) until B_e reached −2.0 T.

Examples of field distribution, $B(z)$, measured at a temperature of 59 K, are shown in Fig. 8. We found a typical periodic field distribution as expected. As B_e was decreased, the field amplitude grew, while the field offset was reduced. After B_e reached 0.2 T, the amplitude growth stopped, meaning that magnetization of the HTSCs saturated. It was found that the SCPMU of type A would be realised by setting $B_e \simeq -0.5$ T to eliminate the field offset.

Let us define the peak-to-peak field amplitude B_a and field offset B_o at the second period as

$$B_a = B(0) - [B(-\lambda_u/2) + B(\lambda_u/2)]/2,$$
$$B_o = B(0) + [B(-\lambda_u/2) + B(\lambda_u/2)]/2.$$

The field amplitude B_a gives the peak field of the SCPMU to be realised under the same conditions (same HTSC material, λ_u = 10 mm, gap = 2 mm).

Fig. 9 shows B_a and B_o as functions of B_e at different temperatures. As expected, operation at a lower temperature results in a stronger field. For example, B_a reaches 1.5 T at 50 K and $B_e = -2$ T. It should be noted that a $|B_e|$ value of 2 T is not sufficient for saturation at 50 K. We can expect a larger B_a (*i.e.* peak field) by applying a higher B_e, which was not possible in the experiment because the capacity of the electromagnet was not enough. As for the field offset elimination, we found an optimum value of B_e at each temperature.

4. Discussion

We have successfully demonstrated the principle of the SCPMU scheme in the experiments described in the preceding section. The important point in this scheme is that bulk-type HTSCs can be utilized, which allows a much higher operating temperature than in the IDs driven by superconducting coils operating around liquid-helium temperature. For example, it was found that the HTSC used in the experiments had a j_c value of 2 kA mm^{-2} at 35 K. Substituting $\lambda_u = 15$ mm, $j_c = 2$ kA mm^{-2} and $g = 3$ mm into equation (1), we have a peak field of 4 T, which is about three times higher than that achieved in the REPM undulator (Tanaka, Shirasawa *et al.*, 2004).

In this paper we have discussed the application of SCPMs to a short-period undulator. It should be noted, however, that the SCPMU scheme can also be applied to the construction of a wiggler that has an extremely strong peak field with a periodic length much shorter than those of wigglers driven by superconducting coils. For example, a SCPM with a peak field of 17 T at a temperature of 29 K has been developed in Japan (Tomita & Murakami, 2003). It has a cylindrical shape with a diameter of 26.5 mm and a thickness of 15 mm. Using such SCPMs it will be possible to construct a wiggler with a peak field above 10 T and a periodic length shorter than 30 mm. Needless to say, reducing the periodic length leads to a larger number of periods, resulting in a higher brightness of synchrotron radiation.

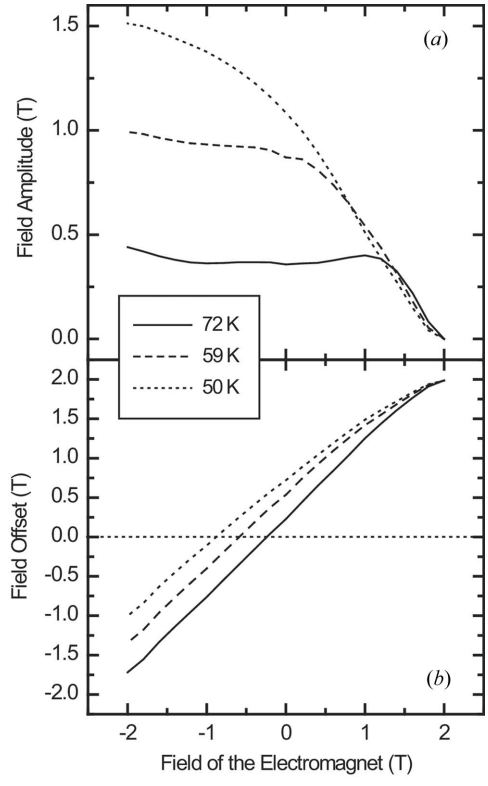

Figure 9
Dependences of the field profile on the applied field strength in terms of (*a*) amplitude and (*b*) offset at the second period for different temperatures.

As described so far, the SCPMU has a great potential to extend the capability of synchrotron radiation sources. It should be noted, however, that there are a number of technical challenges to be overcome for realisation of SCPMUs.

Firstly, a strong uniform field should be supplied to magnetize the HTSCs. It may be necessary to adopt (low-temperature) superconducting coils, which in turn makes the entire device very complicated.

Secondly, the field correction technique should be developed. The *in situ* sorting (Tanaka *et al.*, 2001), essentially reassembling the magnet pieces to reduce the phase error and integrated multipole, is one candidate because the structure of the SCPMU is similar to that of the REPM undulator (both consist of arrays of permanent magnets). In addition, the uniformity of j_c values should be good enough. In the case of REPMs, the manufacturer can supply products with remanent field errors of 1% in magnitude and 1° in angle. Requirements on the j_c values of SCPMs will be similar to those on the REPMs.

Thirdly, the performance of the magnetic field will be affected by changing the gap to tune the photon energy, which should be carefully investigated.

Finally, the operating temperature of the SCPMs should be determined, taking several factors into account: the safety margin of the j_c values, cooling capacity of the cryocooler, and resistive heating by the electron beam.

APPENDIX *A*
Calculation of magnetic fields generated by regularly placed coils

Here we calculate the magnetic field generated by infinitely long coils placed regularly as shown in Fig. 10. First, we consider the case when $a \to 0$ and $b \to 0$ with the current I inside the coil being kept constant. The current density distribution in such coils is expressed as

$$j(\xi = z + iy) = I \sum_{n=-\infty}^{\infty} \delta[\, y - (g/2)] \times \left\{\delta\left[z - \left(n + \tfrac{1}{4}\right)\lambda_u\right] - \delta\left[z - \left(n - \tfrac{1}{4}\right)\lambda_u\right]\right\}.$$

The magnetic field generated in the yz plane is expressed by the two-dimensional form of Biot–Savart's law (Halbach, 1980),

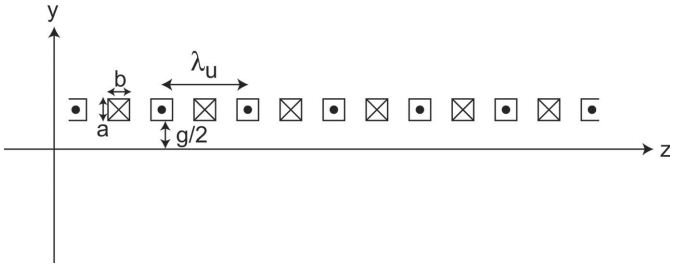

Figure 10
Magnetic field generated by coils placed regularly.

$$B^*(\xi) = B_y(\xi) - iB_z(\xi) = \frac{\mu_0}{2\pi i}\int \frac{j(\xi')}{\xi - \xi'}\,\mathrm{d}y\,\mathrm{d}z, \qquad (2)$$

where μ_0 is the permeability of a vacuum.

Because $j(\xi)$ is periodic along the z axis, it can be expanded into a Fourier series,

$$j(\xi) = \delta[\,y - (g/2)]\left[(4/\lambda_u)\sum_{n=0}^{\infty}(-1)^n \sin(2n+1)k_u z\right], \qquad (3)$$

with $k_u = 2\pi/\lambda_u$. Substituting (3) into (2), we have the vertical magnetic field b_y generated by the infinitely fine coils,

$$b_y(\xi) = (2\mu_0/\lambda_u)\sum_{n=0}^{\infty}(-1)^n \exp\big[-(2n+1)\,k_u|y-(g/2)|\big] \times \cos\big[(2n+1)k_u z\big]. \qquad (4)$$

Now let us consider the case when a and b have finite values. The magnetic field in such a case is calculated by integrating (4) over the cross-sectional area of the coil,

$$B_y(y,z) = \frac{1}{ab}\int_{g/2}^{b+g/2}\int_{-a/2}^{a/2} b_y(y-y', z-z')\;\mathrm{d}y'\,\mathrm{d}z'.$$

Substituting (4) into the above equation and assuming $y < g/2$, we have

$$B_y(y,z) = \frac{2\mu_0 I}{\lambda_u}\sum_{n=0}^{\infty}(-1)^n\;\frac{\sin(n+\frac{1}{2})\,k_u a}{(n+\frac{1}{2})\,k_u a} \times \exp\big[-(n+\tfrac{1}{2})\,k_u(g-2y)\big] \times \frac{1-\exp\big[-(2n+1)\,k_u b\big]}{(2n+1)\,k_u b}\cos(2n+1)\,k_u z. \qquad (5)$$

The magnetic field consists of odd harmonics. Among them, the fundamental component ($n = 0$) is the most dominant and has the peak field B_p on axis ($y = 0$),

$$B_p = \frac{2\mu_0 I}{\lambda_u}\;\frac{1-\exp(-k_u b)}{k_u b}\;\frac{\sin(k_u a/2)}{k_u a/2}\;\exp(-k_u g/2). \qquad (6)$$

The exponential dependence on the gap is identical to that of the REPM undulator with the Halbach configuration.

The authors thank Mr Seike of SPring-8 for supporting the experimental set-up.

References

Chouhan, S., Rossmanith, R., Strohmer, S., Doelling, D., Geisler, A., Hobl, A. & Kubsky, S. (2003). *Proceedings of the 2003 Particle Accelerator Conference, PAC 2003*, pp. 899–901. Piscataway, NJ: IEEE.

Halbach, K. (1980). *Nucl. Instrum. Methods*, **169**, 1–10.

Hara, T., Tanaka, T., Kitamura, H., Bizen, T., Seike, T., Kohda, T. & Matsuura, Y. (2004). *Phys. Rev. ST-AB*, **7**, 050702.

Ingold, G., Solomon, L., Ben-Zvi, I., Krinsky, S., Li, D., Lynch, D., Sheehan, J., Woodle, N., Qiu, X. Z., Yu, L. H., Zhang, X., Sampson, W., Gardner, M., Robins, K., Lehrman, I., Heuer, R., Sheehan, J. & Weissenburger, D. (1993*a*) *Proceedings of the 1993 Particle Accelerator Conference, PAC 1993*, pp. 1439–1441. Piscataway, NJ: IEEE.

Ingold, G., Solomon, L., Ben-Zvi, I., Krinsky, S., Li, D., Lynch, D. R., Sheehan, J., Woodle M. H., Qiu, X. Z., Yu, L. H., Zhang, X., Sampson, W., Garber, M., Robins, K., Lehrman, I. S., Heuer, R., Sheehan, J. R. & Weissenburger, D. (1993*b*). *Proc. SPIE*, **2013**, 68–72.

Koziol, Z. M., Franse, J. J., Chatel, P. F. & Menovsky, A. A. (1994). *Phys. Rev. B*, **50**, 15978–15992.

Sagawa, M., Fujimura, S., Yamamoto, H., Matuura, Y. & Hirosawa, S. (1985). *J. Appl. Phys.* **57**, 4094–4096.

Schlueter, R., Marks, S., Prestemon, S. & Dietderich, D. (2004). *Synchrotron Rad. News*, **17**, 33–40.

Tanaka, T., Hara, T., Kitamura, H., Tsuru, R., Bizen, T., Maréchal, X. & Seike, T. (2004). *Phys. Rev. ST-AB*, **7**, 090704.

Tanaka, T., Seike, T. & Kitamura, H. (2001). *Nucl. Instrum. Methods*, A**465**, 600–605.

Tanaka, T., Shirasawa, K., Seike, T. & Kitamura, H. (2004). *Proceedings of the 8th International Conference on Synchrotron Radiation Instrumentation*, AIP Conference Proceedings Volume 705, pp. 227–230. New York: American Institute of Physics.

Tomita, M. & Murakami, M. (2003). *Nature (London)*, **421**, 517–520.

Warren, R. W. & Fortgang, C. M. (1993). *Nucl. Instrum. Methods*, A**331**, 48–51.